

### III-Nitride full-scale high-resolution microdisplays

Jacob Day,<sup>1</sup> J. Li,<sup>2</sup> D. Y. C. Lie,<sup>1</sup> Charles Bradford,<sup>3</sup> J. Y. Lin,<sup>1,a)</sup> and H. X. Jiang<sup>1,b)</sup>

<sup>1</sup>Department of Electrical and Computer Engineering, Texas Tech University, Lubbock, Texas 79409, USA

<sup>2</sup>III-N Technology, Inc., Lubbock, Texas 79416, USA

<sup>3</sup>US Army, RDECOM CERDEC Night Vision and Electronic Sensors Directorate, 10221 Burbeck Road, Fort Belvoir, Virginia 22060, USA

(Received 5 June 2011; accepted 2 July 2011; published online 22 July 2011)

We report the realization and properties of a high-resolution solid-state self-emissive microdisplay based on III-nitride semiconductor micro-size light emitting diodes ( $\mu$ LEDs) capable of delivering *video* graphics images. The luminance level of III-nitride microdisplays is several orders of magnitude higher than those of liquid crystal and organic-LED displays. The pixel emission intensity was almost constant over an operational temperature range from 100 to  $-100^\circ\text{C}$ . The outstanding performance is a direct attribute of III-nitride semiconductors. An energy efficient active drive scheme is accomplished by hybrid integration between  $\mu$ LED arrays and Si CMOS (complementary metal-oxide-semiconductor) active matrix integrated circuits. These integrated devices could play important roles in emerging fields such as biophotonics and optogenetics, as well as ultra-portable products such as next generation pico-projectors. © 2011 American Institute of Physics. [doi:10.1063/1.3615679]

III-Nitride light emitting diodes (LEDs) have achieved dramatic advances alongside developments in indicators and solid-state lighting (SSL).<sup>1</sup> For example, InGaN-based white LEDs have achieved a luminous efficacy of 150 lm/W,<sup>2</sup> much higher than those of other self-emissive devices, such as organic LEDs (OLEDs). With their intrinsic physical properties and low voltage operation characteristics, LEDs have a much longer operational lifetime ( $>100\,000$  h) and can be operated at extreme conditions such as high or low temperatures and humidity. These properties make LEDs an ideal candidate for applications where performance, reliability, and lifetime are critical. Since their inception,<sup>3–5</sup>  $\mu$ LEDs have emerged as a promising technology for many applications, including self-emissive microdisplays,<sup>5–8</sup> single-chip high voltage AC-LEDs for SSL,<sup>9–11</sup> and light sources for optogenetic neuromodulation.<sup>12–15</sup> The InGaN-based  $\mu$ LED array has also opened avenues for multi-site photostimulation of neuron cells and offers the opportunity to probe biological neuron networks at the network level.<sup>12,13</sup> In particular, III-nitride  $\mu$ LED based self-emissive microdisplays have the potential to provide high brightness, contrast, resolution, and reliability, and long-life, compactness, operation under harsh conditions, and under bright daylight—properties which cannot be matched by more conventional liquid crystal display (LCD), OLED, digital light processing (DLP), and laser beam steering (LBS) based microdisplay technologies.<sup>16,17</sup>

Until now, microdisplays based on semiconductors that are capable of delivering *video* graphics images have not been realized. There have been several reports on monolithic III-nitride  $\mu$ LED arrays.<sup>5–8</sup> In a monolithic microdisplay,  $\mu$ LED and the signal transmission paths, including all of the metal lines for n- and p-type contacts, are integrated on the same GaN wafer. The device requires a separate driving circuit to operate. However, to achieve a full-scale microdisplay in a

monolithic  $\mu$ LED array, connecting the huge amount of control signals from a separate driving circuit to the microdisplay within a limited space, is a very difficult if not impossible task. Moreover, such a monolithic  $\mu$ LED microdisplay can only be driven in the passive mode. In this mode, one can only independently access one row at a time, and a high source voltage is required because an entire pixel column is driven in series while the appropriate  $\mu$ LED is turned on or off using row addressing. For high-resolution video displays, or for very high luminance-requirement sunlight readable displays, the efficiency and thermal dissipation become serious issues.<sup>16</sup> Here, we report the realization of energy efficient, high-resolution green and blue solid-state self-emissive microdisplays operating in an active driving scheme. Several advances were the key, which include (1) achieving low contact resistance of  $\mu$ LEDs with 12  $\mu\text{m}$  pixel size; (2) design and fabrication of an active matrix driver integrated circuit (IC) implemented in a digital complementary metal-oxide-semiconductor (CMOS) process; and (3) hybrid integration of InGaN  $\mu$ LED array with Si CMOS IC chip using flip-chip bonding via indium bumps of only 6  $\mu\text{m}$  in size.

The  $\mu$ LED layer structure used for microdisplay fabrication shown in Fig. 1(a) was grown on (0001) sapphire substrate by metal-organic chemical vapor deposition. The fabrication steps of  $\mu$ LED arrays (with 12  $\mu\text{m}$  pixel size and 15  $\mu\text{m}$  pitch) were built on previously reported procedures for etching and metallization.<sup>3–11,18</sup> Effective hole injection is always an issue for III-nitride emitters due to the relatively large activation energy of Mg acceptors and low conductivity of p-GaN.<sup>19</sup> Reducing the contact resistance will enhance the hole injection efficiency, reduce threshold current and heat generation, and increase the device operating lifetime. For improved performance, we have adopted a heavily Mg doped p-type GaN ( $\text{p}^+$ -GaN) layer as the contact layer to minimize the contact resistance.<sup>20</sup> The operating voltages of individual  $\mu$ LEDs are comparable to those of conventional broad-area ( $300 \times 300 \mu\text{m}^2$ ) green and blue LEDs,<sup>19</sup> CMOS

<sup>a)</sup>Electronic mail: jingyu.lin@ttu.edu.

<sup>b)</sup>Electronic mail: hx.jiang@ttu.edu.

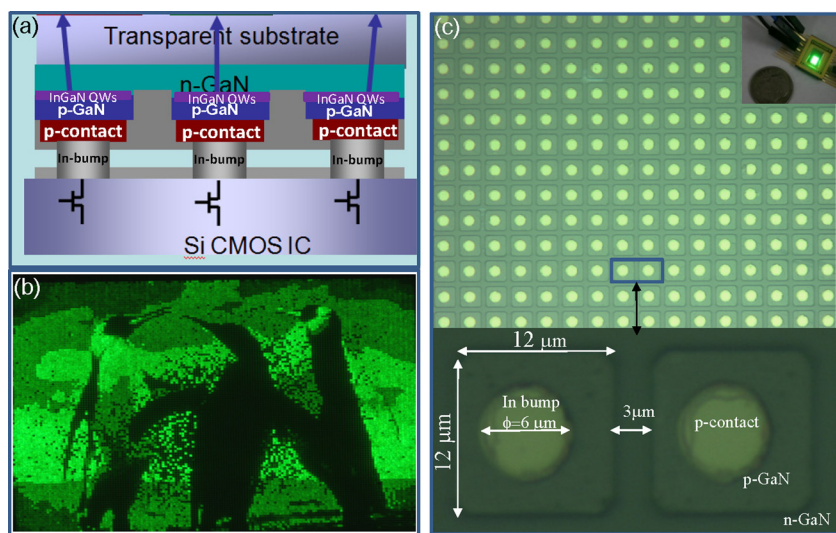


FIG. 1. (Color online) (a) Illustration of flip-chip bonding between  $\mu$ LED matrix array and CMOS driver IC via indium bumps to form a highly integrated microdisplay in one package. (b) A grayscale projected image of penguins from a green (517 nm) InGaN microdisplay (having a pixel size of  $12 \mu\text{m}$  and a pitch distance of  $15 \mu\text{m}$ ) operating at a driving current of  $1 \mu\text{A}$  per pixel. (c) The zoom-in image of a segment of an InGaN  $\mu$ LED array chip showing  $\mu$ LED pixels and indium bumps viewed from the transparent sapphire side. The top inset shows a fully assembled green InGaN microdisplay ( $160 \times 120$  pixels) in operation ( $1 \mu\text{A}$  per pixel).

active matrix  $640 \times 480$  and  $160 \times 120$  microdisplay controller ICs having a  $\mu$ LED current of  $0.5 \mu\text{A}$  to  $10 \mu\text{A}$  and the same pitch ( $15 \mu\text{m}$ ) as the  $\mu$ LED array have been designed and fabricated in a CMOS process. An active matrix display means that each pixel is geared with its own driver circuit in CMOS that is capable of storing data and driving each individual  $\mu$ LED. The integration between the  $\mu$ LED array and Si CMOS driver IC was accomplished by flip-chip bonding using indium bumps, which were deposited by thermal evaporation. The pixels share a common anode (n-type contact) with an independently controllable cathode (p-type contact). The hybrid integration means that thousands of signal connections between the microdisplay and the driving IC have been established in a single flip-chip bonding package.

The inset of Fig. 1(b) shows a fully assembled InGaN microdisplay. Figure 1(b) reveals that the fabricated microdisplays are capable of delivering real time video graphics

images. To illustrate more details of the fabricated devices, we show an expanded view of a segment of a  $\mu$ LED array chip in Fig. 1(c). Micro-LED pixels and indium metal bumps deposited on the  $\mu$ LED pixels are clearly seen from the transparent sapphire side. The results demonstrate  $\sim 6 \mu\text{m}$  indium bumps with excellent size uniformity. Figure 2 shows the measured characteristics of InGaN  $\mu$ LED pixels. The nearly linear optical power output with increasing forward current will be very useful for a range of applications and also ensures high brightness with a large dynamic gray scale range. The  $L-I$  (optical output power vs forward driving current) characteristics of individual pixels within a microdisplay have been measured. For  $I \leq 1 \text{ mA}$ , the variation in emission intensity among different pixels is negligible.<sup>5</sup> To obtain a sense of brightness, we characterized the luminance of the green  $\mu$ LED pixels. As shown in Fig. 3(a), a  $12 \mu\text{m}$  pixel outputs roughly  $1 \text{ mcd}/\mu\text{A}$  and the luminance increases almost linearly with  $I$  for  $I < 100 \mu\text{A}$ . For a microdisplay with a pitch distance of  $15 \mu\text{m}$ , when every pixel within the array is lit up and operates at  $1 \mu\text{A}$ , the brightness of the microdisplay can be calculated to be  $\sim 4 \times 10^6 \text{ cd}/\text{m}^2$ . This luminance level is several orders of magnitude higher than those of LCD and OLEDs. Based on the pixel characteristics in Fig. 2, at  $I = 1 \mu\text{A}$ , a green  $\mu$ LED pixel has a voltage of around 2.6 V. This means that the power dissipation within the  $\mu$ LED array is only about 0.8 W for a full VGA ( $640 \times 480$  pixels)

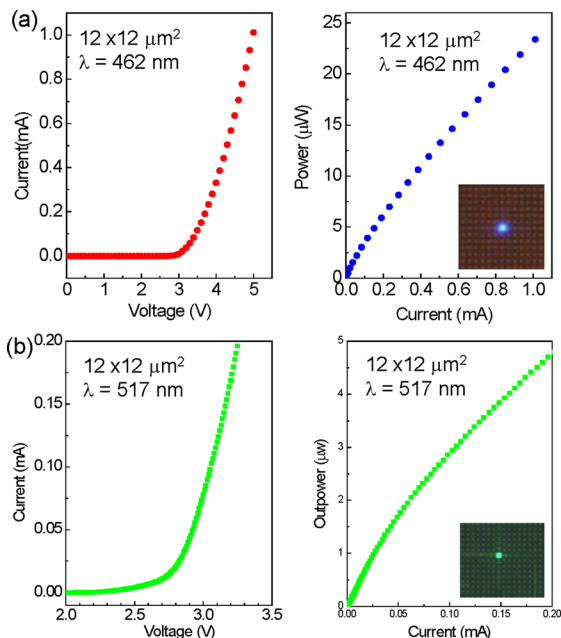


FIG. 2. (Color online) I-V and L-I characteristics of (a) blue (462 nm) and (b) green (517 nm)  $\mu$ LED pixels. The optical power was measured by a calibrated optical power meter placed on the sapphire side of a  $\mu$ LED array when a single pixel was lit.

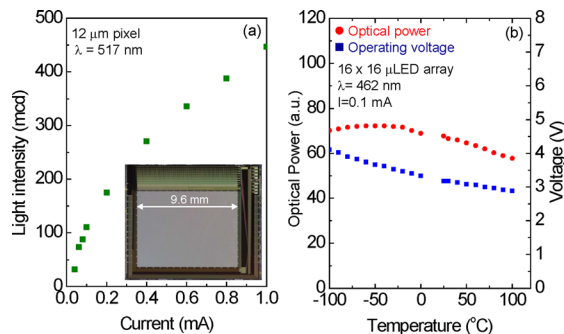


FIG. 3. (Color online) (a) Luminance of a single green (517 nm)  $\mu$ LED pixel as a function of driving current and the inset shows a micrograph of a fully assembled video graphics array (VGA) microdisplay ( $640 \times 480$  pixels). (b) The temperature dependence of the relative emission optical power of an InGaN  $\mu$ LED array.

TABLE I. Comparison among various technologies for microdisplays.

Technology	Liquid crystal	Organic LED	III-Nitride $\mu$ LED	Digital light processing	Laser beam steering
Mechanism	Backlighting/LED	Self-emissive	Self-emissive	Backlighting/LED	Backlighting/LD
Luminous efficacy	Medium	Low	High	High	High
Luminance	3000 cd/m <sup>2</sup> (full color) ~10 <sup>4</sup> cd/m <sup>2</sup> (green)	1500 cd/m <sup>2</sup> (full color) ~10 <sup>3</sup> cd/m <sup>2</sup> (yellow)	~10 <sup>5</sup> cd/m <sup>2</sup> (full color) ~10 <sup>7</sup> cd/m <sup>2</sup> (blue/green)	~1000 cd/m <sup>2</sup> (full color)	~1000 cd/m <sup>2</sup> (full color)
Contrast ratio	200:1 (intrinsic)	Very high >10 000:1	Very high > 10 000:1	High	High
Response time	ms	$\mu$ s	ns	ms	ms
Operating temperature	0 to 60 °C requires heater	-50 to 70 °C	-100 to 120 °C	To be determined	To be determined
Shock resistance	Low	Medium	High	Medium	Medium
Lifetime	Medium	Medium	Long	Medium (limited by MEMS)	Short (limited by laser diodes)
Cost	Low	Low	Low	High	High

microdisplay if every pixel within the  $\mu$ LED array is lit up simultaneously. This estimate represents the upper limit of power dissipation since normally only a fraction (~25%) of pixels are lit up for graphical video image displays. Notice also that 1  $\mu$ A driving current translates to a current density of about 0.7 A/cm<sup>2</sup> for a 12  $\mu$ m pixel, which is about 1/30 of the typical value (22 A/cm<sup>2</sup>) in conventional indicator LEDs, which have an average chip size of 300  $\mu$ m  $\times$  300  $\mu$ m and an expected operating lifetime exceeding 100 000 h under normal operating conditions (i.e.,  $I=20$  mA). These estimates also imply that the lifetime of III-nitride microdisplays should be as long as those of indicator LEDs.

The operating temperature ( $T$ ) dependence of the optical output power of our  $\mu$ LEDs has been measured, and the results are depicted in Fig. 3(b). The intensity of the  $\mu$ LED emission decreased by about 10% when  $T$  was raised from room temperature to +100 °C and remained almost constant when  $T$  was cooled down from room temperature to -100 °C, while the operating voltage at 0.1 mA varied from 4.1 V at -100 °C to 2.9 V at +100 °C. This continuous reduction in the operating voltage with increasing  $T$  is due to thermal activation of free holes ( $p$ ) described by the process of  $p \sim \exp(-E_A/kT)$ , where the Mg acceptor activation energy ( $E_A$ ) in GaN is about 160 meV. The  $T$  dependence of the  $\mu$ LED emission intensity in Fig. 3(b) represents the lowest thermal quenching ever reported for any type of microdisplay. The outstanding thermal stability is a direct attribute of III-nitride semiconductors.

Unique features of III-nitride microdisplays are summarized in Table I. Unlike LCDs, which normally require an external light source, III-nitride microdisplays are self-emissive and result in the saving of both space and power and allow viewing from any angle without color shift and degradation in contrast. On the other hand, OLEDs must be driven at current densities many orders of magnitude lower than semiconductor LEDs to obtain devices with a reasonable lifetime and hence are not suitable for high-intensity use. DLP and LBS devices require the use of rapidly scanning microelectromechanical (MEMS) mirrors and separate light sources such as LEDs or laser diodes (LDs), which adds complexity, volume, and cost to the devices. Moreover, the service lifetimes of MEMS and LDs are shorter than those of LEDs. Based on time-resolved electroluminescence measurement, III-nitride  $\mu$ LEDs have a fast response, on the order of 0.2 ns.<sup>4</sup> This

property opens up their potential uses as light sources for site selective fluorescence lifetime studies. The present study clearly demonstrated that III-nitride microdisplays are a favorable competing technology compared to LCD, OLED, DLP, and LBS for ultra-portable products such as next generation pico-projectors, wearable displays, and head-up displays.

This work is supported by ARMY contract No. W909MY-09-C-0014. We thank Sixuan Jin and Weiping Zhao for their skillful help with lithography and device processing. We gratefully acknowledge useful discussions with Zhaoyang Fan. Lin and Jiang are grateful to the AT&T Foundation for the support of Ed Whitacre and Linda Whitacre Endowed chairs.

- <sup>1</sup>A. Bergh, G. Crawford, A. Duggal, and R. Haitz, *Phys. Today* **54**(December), 42 (2001).
- <sup>2</sup>Y. Narukawa, M. Sano, M. Ichikawa, S. Minato, T. Sakamoto, T. Yamada, and T. Mukai, *Jpn. J. Appl. Phys.* **46**, L963 (2007).
- <sup>3</sup>S. X. Jin, J. Li, J. Z. Li, J. Y. Lin, and H. X. Jiang, *Appl. Phys. Lett.* **76**, 631 (1999).
- <sup>4</sup>S. X. Jin, J. Li, J. Shakya, J. Y. Lin, and H. X. Jiang, *Appl. Phys. Lett.* **78**, 3532 (2001).
- <sup>5</sup>H. X. Jiang, S. X. Jin, J. Li, J. Shakya, and J. Y. Lin, *Appl. Phys. Lett.* **78**, 1303 (2001).
- <sup>6</sup>H. X. Jiang, S. X. Jin, J. Li, and J. Y. Lin, U.S. patent 6,410,940 (2002).
- <sup>7</sup>H. X. Jiang and J. Y. Lin, *CRC Crit. Rev. Solid State Mater. Sci.* **28**, 131 (2003).
- <sup>8</sup>J. J. D. McKendry, B. R. Rae, Z. Gong, K. R., Muir, B. Guilhabert, D. Massoubre, E. Gu, D. Renshaw, M. D. Dawson, and R. K. Henderson, *IEEE Photon. Technol. Lett.* **21**, 811 (2009).
- <sup>9</sup>H. X. Jiang, J. Y. Lin, and S. X. Jin, U.S. patent 6,957,899 (2005) and 7,221,044 (2007).
- <sup>10</sup>Z. Y. Fan, J. Li, J. Y. Lin, and H. X. Jiang, U.S. patent 7,714,348 (2010).
- <sup>11</sup>Z. Y. Fan, H. X. Jiang, and J. Y. Lin, *J. Phys. D: Appl. Phys.*, **41** 094001 (2008).
- <sup>12</sup>V. Poher, N. Grossman, G. T. Kennedy, K. Nikolic, H. X. Zhang, Z. Gong, E. M. Drakakis, E. Gu, M. D. Dawson, P. M. W. French, P. Degenaar, and M. A. Neil, *J. Phys. D: Appl. Phys.* **41**, 094014 (2008).
- <sup>13</sup>N. Grossman, V. Poher, M. S. Grubb, G. T. Kennedy, K. Nikolic, B. McGovern, P. R. Berlinguer, Z. Gong, E. M. Drakakis, M. A. Neil, M. D. Dawson, J. Burrone, and P. Degenaar, *J. Neural Eng.* **7**, 016004 (2010).
- <sup>14</sup>P. Degenaar, N. Grossman, M. Memon, J. Burrone, M. D. Dawson, E. Drakakis, M. A. Neil, and K. Nikolic, *J. Neural Eng.* **6**, 035007 (2009).
- <sup>15</sup>T. Young and C. Chen, *Biomaterials* **27**, 3361 (2006).
- <sup>16</sup>W. E. Howard and O. F. Prache, *IBM J. Res. Dev.* **45**, 115 (2001).
- <sup>17</sup>D. Vettese, *Nat. Photon.* **4**, 752 (2010).
- <sup>18</sup>S. J. Pearton, J. C. Zolper, R. J. Shul, and F. Ren, *J. Appl. Phys.* **86**, 1 (1999).
- <sup>19</sup>S. Nakamura, S. J. Pearton, and G. Fasol, *G. Meas. Sci. Technol.* **12**, 755 (2001).
- <sup>20</sup>J. Dennemarck, T. Böttcher, S. Figge, S. Einfeldt, R. Kröger, D. Hommel, E. Kaminska, W. Wiatroszak, and A. Piotrowska, *Phys. Status Solidi C* **1**, 2537 (2004).